Altered State Dependence of C-Type Inactivation in the Long and Short Forms of Human Kv1.5

Harley T. Kurata, Gordon S. Soon, and David Fedida

Department of Physiology, University of British Columbia, Vancouver, British Columbia, V6T 1Z3, Canada

ABSTRACT Evidence from both human and murine cardiomyocytes suggests that truncated isoforms of Kv1.5 can be expressed in vivo. Using whole-cell patch-clamp recordings, we have characterized the activation and inactivation properties of Kv1.5ΔN209, a naturally occurring short form of human Kv1.5 that lacks roughly 75% of the T1 domain. When expressed in HEK 293 cells, this truncated channel exhibited a $V_{1/2}$ of -19.5 ± 0.9 mV for activation and -35.7 ± 0.7 mV for inactivation, compared with a $V_{1/2}$ of -11.2 ± 0.3 mV for activation and -0.9 ± 1.6 mV for inactivation in full-length Kv.15. Kv1.5ΔN209 channels exhibited several features rarely observed in voltage-gated K^+ channels and absent in full-length Kv1.5, including a U-shaped voltage dependence of inactivation and "excessive cumulative inactivation," in which a train of repetitive depolarizations resulted in greater inactivation than a continuous pulse. Kv1.5ΔN209 also exhibited a stronger voltage dependence to recovery from inactivation, with the time to half-recovery changing e-fold over 30 mV compared with 66 mV in full-length Kv1.5. During trains of human action potential voltage clamps, Kv1.5ΔN209 showed 30–35% greater accumulated inactivation than full-length Kv1.5. These results can be explained with a model based on an allosteric model of inactivation in Kv2.1 (Klemic, K.G., C.-C. Shieh, G.E. Kirsch, and S.W. Jones. 1998. *Biophys. J.* 74:1779–1789) in which an absence of the NH_2 terminus results in accelerated inactivation from closed states relative to full-length Kv1.5. We suggest that differential expression of isoforms of Kv1.5 may contribute to K^+ current diversity in human heart and many other tissues.

KEY WORDS: potassium channel • Kv1.5 • gating • inactivation • NH_2-terminal deletion

INTRODUCTION

The Kv1.5 (KCNA5) channel is a mammalian homologue of *Shaker* that is widely expressed throughout the cardiovascular system and elsewhere. It is found in human adult and fetal hearts (Tamkun et al., 1991; Fedida et al., 1993), in mouse and rabbit heart (Attali et al., 1993; Sasaki et al., 1995; Dobrzynski et al., 2000), in vascular and intestinal smooth muscles (Overturf et al., 1994; Clément-Chomienne et al., 1999), and also in airways (Adda et al., 1996). The homomeric channel expresses as a rapidly activating delayed rectifier K^+ current with an intermediate rate of inactivation, which is modulated by the activity of β subunits (Sewing et al., 1996). In excitable tissues, this channel is often proposed to have an important function during repolarization in the termination of excitation events, which has been best defined in human atrium (Wang et al., 1993; Schaffer et al., 1998), and vascular smooth muscle. Clinically, downregulation of the channel may play a role in the ionic remodeling that accompanies disease states like atrial fibrillation and hypertension (Van Wagoner et al., 1997; Brandt et al., 2000).

Address correspondence to Dr. David Fedida, Department of Physiology, University of British Columbia, 2146 Health Sciences Mall, Vancouver, British Columbia, V6T 1Z3 Canada. Fax: (604) 822-6048; E-mail: fedida@interchange.ubc.ca

What is less generally appreciated is that Kv1.5 channels, like KvLQT1 (Jiang et al., 1997), appear to exist in at least two isoforms in murine and human cardiac myocytes. An in-frame start codon corresponding to residue M210 in the long form of the channel provides the mechanism for expression of NH_2 terminally truncated short forms of the channel. In the mouse, it appears that these isoforms arise from an unusual splicing mechanism within the exonic structure of the Kv1.5 gene (Attali et al., 1993). In addition, it has been recently suggested that posttranslational proteolysis can result in the generation of tetrameric NH_2 terminally truncated channels in mammalian cells (Strang et al., 2001). Northern blot analysis has also previously revealed two distinct bands of Kv1.5 RNA of appropriate size in human atrium, both neonatal and adult (Tamkun et al., 1991; Fedida et al., 1993). At the present time, it is not entirely clear which isoforms of the channel, the long or short, and in what proportion, underlie the phenotypic current usually observed because the biophysical properties of the short form of Kv1.5 have not been examined.

The region of the NH_2 terminus that is absent in the short form of the channel is important for a number of fundamental properties. The first 200 amino acids mediate the interaction of the channel with β subunits (Rehm and Lazdunski, 1988; Rettig et al., 1994; Sewing

et al., 1996; Pongs et al., 1999) that alter the extent and rate of inactivation in this channel. Within this region the T1 domain is a highly conserved cytoplasmic NH_2-terminal region of voltage-gated K^+ channels, ~100 amino acids in length. The T1 domain has been shown to prevent heteromultimerization of different Kv channel subfamilies (Li et al., 1992; Shen and Pfaffinger, 1995; Xu et al., 1995). However, it is now known that the T1 domains are not absolutely required for channel assembly, as T1 deletion mutants of Kv2.1 (VanDongen et al., 1990), *Shaker*, Kv1.3, Kv1.4, and Kv1.5 have all been shown to assemble into functional channels (Lee et al., 1994; Tu et al., 1996; Fedida et al., 1999; Kobertz and Miller, 1999). The T1 domain also influences channel gating, as several studies have shown that deletion mutations and point mutations in the NH_2 terminus can substantially alter the voltage dependence and kinetics of channel activation (Kobertz and Miller, 1999; Cushman et al., 2000; Minor et al., 2000). However, the mechanism by which these effects arise remains uncertain. Structures determined for several mutated forms of the T1 domain suggest that interactions between polar amino acids in T1 exert strong effects on the stability of the closed-state of the channel (Minor et al., 2000). Further, recent crystallographic and biochemical evidence suggests that, in intact channels, the T1 domain tetramerizes and adopts a "hanging gondola" structure, away from the inner mouth of the pore (Kreusch et al., 1998; Gulbis et al., 2000; Kobertz et al., 2000).

Despite their long NH_2-terminal sequence, Kv1.5 channels have no NH_2-terminal ball structure, and are thought to inactivate by slower mechanisms that which we group together here under the term "C-type mechanism" (Fedida et al., 1999). This mode of inactivation is typically much slower than N-type inactivation, although the rates of C-type inactivation can vary by several orders of magnitude between different Kv families (Olcese et al., 1997; Jerng et al., 1999). The conformational changes associated with C-type inactivation are believed to involve cooperative constriction of the outer mouth of the channel pore after evacuation of K^+ ions from the permeation pathway (Ogielska et al., 1995; Panyi et al., 1995; Baukrowitz and Yellen, 1996), and the rate can be modulated by mutations to certain pore residues and by the extracellular K^+ concentration (Hoshi et al., 1991; Lopez-Barneo et al., 1993; Ogielska et al., 1995; Panyi et al., 1995).

In this study, we have characterized the gating properties of the short NH_2-terminal form of human Kv1.5. Our study shows that the NH_2 terminus of Kv1.5 exerts effects on both channel activation and inactivation. Of particular interest was that the lack of the NH_2 terminus resulted in a U-shaped voltage dependence of C-type inactivation. We show that this is related to a shift in the state dependence of channel inactivation toward inactivation from closed states, and we believe that this is the first characterization of modulation of C-type inactivation by the NH_2 terminus of a *Shaker* family K^+ channel.

MATERIALS AND METHODS

Cell Preparation and Transient Transfection

All cells were grown in MEM with 10% FBS, at 37°C in an air/5% CO_2 incubator. Unless otherwise noted, HEK 293 cell lines stably expressing full-length human Kv1.5 or the short form of human Kv1.5, hKv1.5ΔN209, were used in all experiments. The Kv1.5ΔN209 short form was generated by removal of the NcoI-NcoI fragment of Kv1.5 (see Fig. 1 A). HEK 293 cells were stably transfected with full-length hKv1.5 or Kv1.5ΔN209 cDNAs using LipofectACE reagent (Canadian Life Technologies).

In some experiments, a Mouse *ltk-* (L) cell line was used as a transient expression system due to its lack of endogenous voltage-gated K^+ channel subunits. 1 d before transfection, cells were plated on glass coverslips in 35-mm petri dishes with 20–30% confluence. On the day of transfection, cells were washed once with MEM with 10% FBS. To identify the transfected cells efficiently, channel DNA was cotransfected with the vector pHook-1 (Invitrogen). This plasmid encodes the production of an antibody to the hapten phOX which, when expressed, is displayed on the cell surface. Channel DNA was mixed with pHook-1 (1:1 ratio, 1 μg each) and 2 μl of LipofectAMINE 2000 (Canadian Life Technologies) in 100 μl of serum-free media, and then added to the dishes containing mouse L cells. Cells were allowed to grow overnight before recording. 1 h before experiments, cells were treated with beads coated with phOX. After 15 min, excess beads were washed off with cell culture medium, and cells that had beads stuck to them were used for electrophysiological recordings.

Solutions

Patch pipettes contained the following (in mM): 5 NaCl, 135 KCl, 4 Na_2ATP, 0.1 GTP, 1 $MgCl_2$, 5 EGTA, and 10 HEPES (adjusted to pH 7.2 with KOH). The bath solution contained the following (in mM): 135 NaCl, 5 KCl, 10 HEPES, 2.8 sodium acetate, 1 $MgCl_2$, and 1 $CaCl_2$, (adjusted to pH 7.4 with NaOH). All chemicals were from Sigma-Aldrich.

Electrophysiological Procedures

Coverslips containing cells were removed from the incubator before experiments and placed in a superfusion chamber (volume 250 μl) containing the control bath solution at 22–23°C, and perfused with bathing solution throughout the experiments. Whole-cell current recording and data analysis were done using an Axopatch 200A amplifier and pClamp 8 software (Axon Instruments). Patch electrodes were fabricated using thin-walled borosilicate glass (World Precision Instruments). Electrodes had resistances of 1–3 MΩ when filled with control filling solution. Capacity compensation and 80% series resistance compensation were used in all whole-cell recordings. The mean capacitance and series resistance from 82 cells studied was 16.2 ± 0.6 pF and 2.4 ± 0.1 MΩ (before series resistance compensation). No leak subtraction was used when recording currents, and zero current levels are denoted by the dotted lines in the current tracings. Data were sampled at 10–20 kHz and filtered at 5–10 kHz. Membrane potentials have not been corrected for small junctional potentials between bath and pipette solutions. Throughout the text, data are shown as mean ± SEM, and tests for significance between two groups were performed using *t* test.

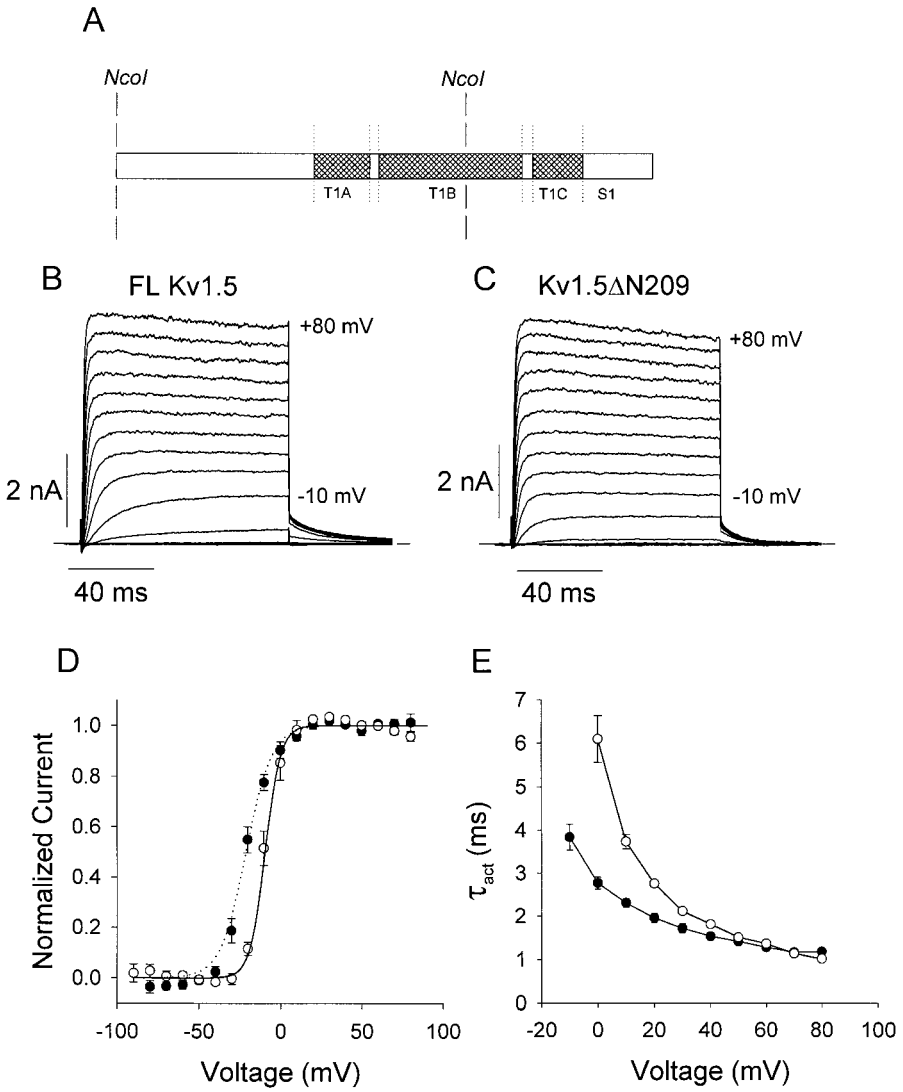

FIGURE 1. Activation properties of Kv1.5ΔN209. (A) The Kv1.5ΔN209 construct was generated by deleting sequence between the two NcoI restriction enzyme sites within Kv1.5. S1 denotes the first transmembrane domain as determined by hydropathy analysis. Activation curves were measured in HEK 293 cells stably expressing (B) full-length (FL) Kv1.5 or (C) Kv1.5ΔN209. Cells were stepped to voltages between −80 and +80 mV in 10-mV steps for 100 ms, followed by a 20-ms repolarization to −40 mV. (D) Tail current amplitudes were normalized and fit with single Boltzmann equations (○, full-length; ●, Kv1.5ΔN209). The $V_{1/2}$ was −11.2 ± 0.3 mV in full-length Kv1.5 and −20.9 ± 1.6 mV in Kv1.5ΔN209 (n = 5). The slope factor, k, was 4.3 ± 1 in full-length Kv1.5 and 7.9 ± 1.6 in Kv1.5ΔN209. (E) Time constants of activation were determined at various potentials by fitting the major part of the activation time courses with single exponential equations (○, full-length; ●, Kv1.5ΔN209).

Data Analysis and Modeling

The voltage dependence of activation and inactivation of Kv1.5 and Kv1.5ΔN209 were fit with Boltzmann functions of the form: $y = 1/(1 + \exp[(V_{1/2} - V)/k])$ and $y = 1/(1 + \exp[(V - V_{1/2})/k]) + C$, respectively, where $V_{1/2}$ represents the voltage at which 50% activation or inactivation occurred, V is the membrane potential, and k is the slope factor that reflects the steepness of the voltage dependence. C represents the fraction of noninactivating channels at potentials where inactivation was most complete. The model was constructed using ScoP and ScoPfit (version 3.51; Simulation Resources), and based on the allosteric model of inactivation proposed by Klemic et al. (1998). The number of channels moving between different states was described by a series of first-order differential equations and solved numerically. The transition rates between horizontal states were exponential functions of voltage of the form: $\text{rate} = k_o \cdot \exp[z_i \cdot e_0 \cdot V/kT]$, where k_o represents the rate at 0 mV, z_i refers to the valency for the transition, and e_0, V, k, and T have their usual meanings. The vertical transitions were assumed to be voltage-independent (see Fig. 8).

RESULTS

Amino Acids 1–209 Modulate the Activation Properties of Kv1.5

The loss of the first 209 amino acid residues in the short form of Kv1.5 corresponds to elimination of the NH_2 terminus nearly to the S1 transmembrane domain, and includes deletion into the T1B domain (Fig. 1 A). The T1A, T1B, and T1C regions correspond to residues 121–150, 156–225, and 233–260 respectively, based on alignments with *Shaker* (Shen et al., 1993; Shen and Pfaffinger, 1995). This does not preclude formation of functional channels, as shown by the presence of such transcripts in human heart (Fedida et al., 1993) and our generation of a stable HEK 293 cell line expressing the short form of Kv1.5 (Kv1.5ΔN209), as well as the expression of T1-deleted channels in *Xenopus oocytes* (Kobertz and Miller, 1999). Currents from Kv1.5ΔN209 appeared very similar to those seen in the

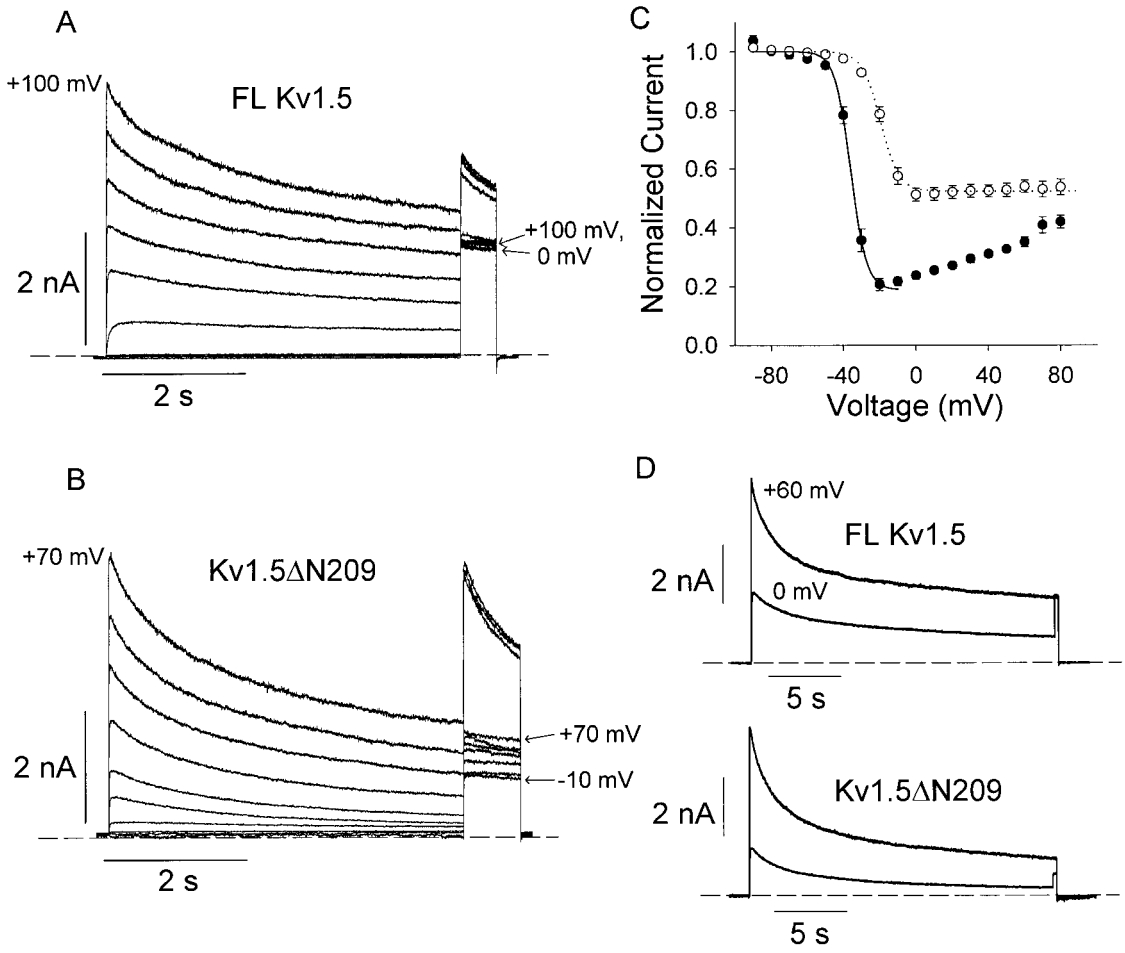

FIGURE 2. Inactivation properties of Kv1.5ΔN209. Inactivation-voltage relationships were measured in HEK 293 cells expressing full-length (FL) Kv1.5 (A) or Kv1.5ΔN209 (B) with a double pulse protocol. Cells were stepped to voltages from −90 up to +100 mV in 20-mV steps for 5 s, followed by a brief test pulse to +60 mV. The size of the test pulse current reflects the number of available (noninactivated) channels. (C) Peak test pulse currents for full-length Kv1.5 (○, $n = 5$) and Kv1.5 ΔN209 (●, $n = 5$), were normalized and fit with single Boltzmann equations. The $V_{1/2}$ was −19.5 ± 0.9 mV in full-length Kv1.5 and −35.7 ± 0.7 mV in Kv1.5ΔN209. k was 5.1 ± 0.8 in full-length channels and 4.3 ± 0.1 in Kv1.5ΔN209. D illustrates current inactivation properties over a longer time scale. Cells were pulsed to either + 60 or 0 mV for 20 s, followed by a brief test pulse to + 60 mV. Dashed lines in this, as in all other figures, denotes the zero current level.

full-length Kv1.5 channels (Fig. 1, B and C), although single exponential fits to the activation time course in Kv1.5ΔN209 reveal slightly faster time constants of activation than in the full-length channel (Fig. 1 E). However, the activation curve of Kv1.5ΔN209 channels does exhibit a leftward shift relative to the full-length channel. The half-activation voltage ($V_{1/2}$) was shifted from −11.2 ± 0.3 mV in full-length Kv1.5 channels ($n = 5$) to −20.9 ± 1.6 mV in Kv1.5ΔN209 ($n = 5$, Fig. 1 D).

Characterization of the Inactivation-voltage Relationship of Kv1.5ΔN209

The most striking differences between the full-length Kv1.5 and the shorter Kv1.5ΔN209 channels are in their respective inactivation properties (Fig. 2). Inactivation-voltage relationships were measured isochronally with a standard double pulse protocol, consisting of a 5-s conditioning pulse to various potentials to inactivate the channel, followed by a brief test pulse to +60 mV, where the conductance-voltage relationship is saturated. Thus, the measured amplitude of the test pulse current is proportional to the number of available (noninactivated) channels. Each double pulse protocol was preceded by a brief 100-ms pulse to +60 mV, which was not long enough to cause further inactivation, but ensured that changes in pipette access resistance and channel run-down during the lengthy protocol did not significantly affect the measured inactivation-voltage relationships. The half-inactivation voltage was shifted from −19.5 ± 0.9 mV in full-length channels to −35.7 ± 0.7 mV in Kv1.5ΔN209. Furthermore, lack of residues 1–209 imparts a dramatic U-shaped voltage dependence to the inactivation-voltage relationship (Fig. 2 C). The inactivating pulses used in these experiments as illustrated in Fig. 2 (A and B) were limited to 5 s, as longer pulses made the completion of the entire protocol impracti-

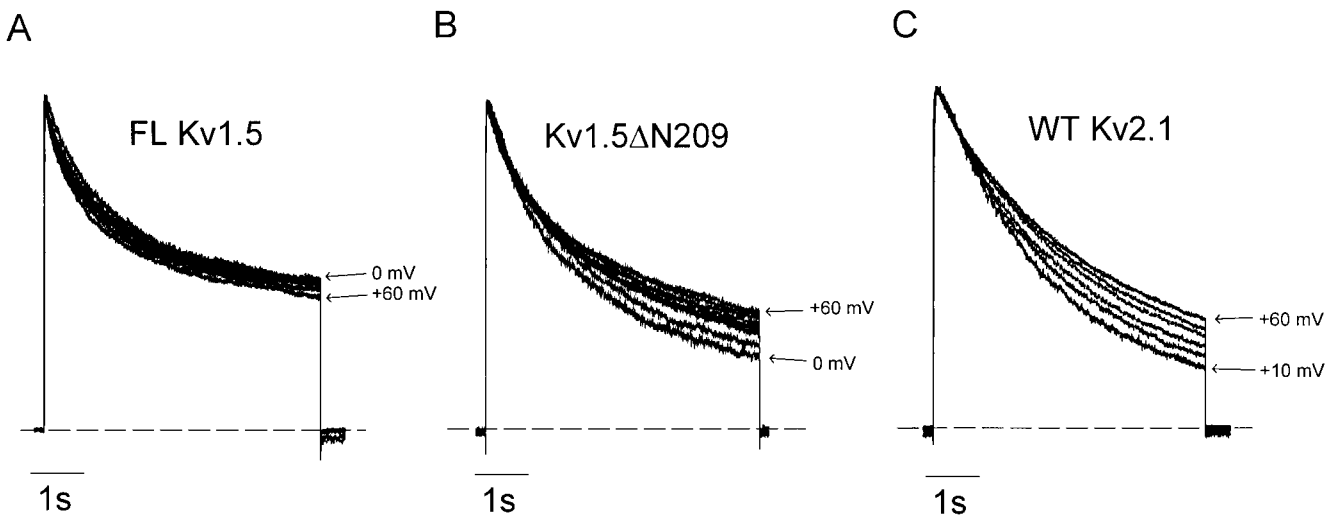

FIGURE 3. Inactivation behavior of full-length Kv1.5, Kv1.5ΔN209, and Kv2.1. Depolarizing pulses to between +60 and 0 mV, 5 s in duration, were applied to HEK 293 cells stably expressing full-length (FL) Kv1.5 (A), Kv1.5ΔN209 (B), or WT Kv2.1 (C). The evoked currents have been normalized to the peak current during each voltage step to illustrate the voltage dependence of the inactivation time course in WT Kv2.1 and Kv1.5ΔN209.

cal. Since inactivation remains incomplete even after depolarizations up to 20 s in duration (Fig. 2 D), the inactivation-voltage relationships presented do not represent a steady state. However, as shown in Fig. 2 D, the observed U-shaped voltage dependence of inactivation is preserved even after 20 s inactivating pulses. Two voltage pulses to +60 and 0 mV were given to full-length Kv1.5 channels (Fig. 2 D, top) and Kv1.5ΔN209 channels (Fig. 2 D, bottom). These were followed by a test pulse to +60 mV to measure the residual current. In the Kv1.5ΔN209 channels, the test pulse current after the 0 mV prepulse falls below that after the +60 mV prepulse. This indicates a U-shaped inactivation-voltage relation in the short form of Kv1.5, which was not observed in full-length channels.

Over the time courses examined, Kv1.5ΔN209 channels appear to inactivate more completely than full-length Kv1.5 channels (Fig. 2, C and D). There is an increase in the maximum level of inactivation during 5-s depolarizations, from a mean of 49 ± 2% to 79 ± 2% in Kv1.5ΔN209. In a previous study of full-length Kv1.5, we have reported that 10-s depolarizations gave a mean reduction of 60% at +60 mV (Fedida et al., 1999), and during the 20-s depolarizations shown in Fig. 2 D the amount of inactivation in full-length channels did not exceed 70%. It appears that the Kv1.5ΔN209 short form can inactivate more completely than the full-length channel, and the half-inactivation voltage of the channel is modified, as well as the overall shape of the inactivation-voltage relationship. These findings suggest alternative or additional pathways for inactivation in the short form of the channel.

As noted, the T1 domains have been implicated in prevention of interfamily subunit heteromultimerization (Shen and Pfaffinger, 1995), and it is known that HEK 293 cells express a small endogenous delayed rectifier K^+ current. In our parent HEK 293cell line, the endogenous current amplitude was ~300 pA at +60 mV so that for the size of currents illustrated in Figs. 1 and 2, 90–95% of the observed current can be accounted for by Kv1.5ΔN209 channel subunits. To confirm that the currents elicited in HEK 293 cells arose from homotetramers of the Kv1.5ΔN209 subunit, as opposed to heterotetramers containing HEK 293 cell endogenous channel subunits, we transiently expressed Kv1.5ΔN209 in Mouse L cells, which showed little or no endogenous voltage-gated K^+ current. The measured inactivation-voltage relationship of Kv1.5ΔN209 exhibited the same features observed in the HEK 293 cell expression system: an upturn of the relationship, and a leftward shift of the half-inactivation voltage. The maximum percent inactivation attained during 5-s pulses is 75.3 ± 3% at −10 mV compared with 46 ± 5% inactivation at +60 mV, the latter value is almost identical with that reached in full-length Kv1.5. The half-inactivation potential is −18.5 ± 1.1 mV in full-length Kv1.5, and shifted to −30.2 ± 0.9 mV in Kv1.5ΔN209. These data support the conclusion that the unique inactivation behavior of Kv1.5ΔN209 is an intrinsic property of the short form of the channel, and is not cell-type dependent or due to heteromultimerization with endogenous channel subunits.

Closed-state Inactivation and Excessive Cumulative Inactivation

The only previous report of a U-shaped voltage dependence of inactivation in Kv channels is for Kv2.1 and its heteromers with Kv5.1 and Kv9.3 (Klemic et al., 1998; Kramer et al., 1998; Kerschensteiner and Stocker,

TABLE I

Inactivation Time Constants for Full-length Kv1.5 and Kv1.5Δ209

	Full-length Kv1.5		Kv1.5ΔN209	
	0 mV	60 mV	0 mV	60 mV
[a]τ_1	1.4 ± 0.2	1.1 ± 0.1	1.5 ± 0.2	1.1 ± 0.1
[a]τ_2	11.7 ± 1.5	9.0 ± 0.9	[b]6.8 ± 0.6	8.8 ± 0.7
a_1	0.32 ± 0.01	0.36 ± 0.02	[b]0.35 ± 0.01	0.34 ± 0.03
a_2	0.43 ± 0.01	0.32 ± 0.02	[b]0.53 ± 0.01	[b]0.44 ± 0.02
c	0.25 ± 0.01	0.30 ± 0.02	[b]0.11 ± 0.01	[b]0.20 ± 0.01

Current decay during 20-s depolarizations to either +60 or 0 mV was fit with a biexponential decay equation ($y = a_1 \cdot \exp(-(t - K)/\tau_1) + a_2 \cdot \exp(-(t - K)/\tau_2 + C)$. Data are mean ± SEM, $n = 4$.

[a]Measured in seconds.

[b]Denotes a significant difference in the Kv1.5ΔN209 column from the corresponding value in full-length Kv1.5, $P < 0.05$.

1999). To explain this relationship, Klemic et al. (1998) proposed a model in which inactivation is favored from late closed states (in which most or all of the voltage sensors are in the activated conformation). One consequence of this model of state-dependent inactivation is that the time course of inactivation during a long voltage step is likely to possess significant voltage dependence. The data in Fig. 3 shows a series of 5-s inactivating pulses in Kv1.5, Kv1.5ΔN209, and Kv2.1, normalized to the peak current at each voltage. The currents evoked in Kv2.1 and Kv1.5ΔN209 are qualitatively very similar, each displaying a highly evident voltage dependence to the observed amount of inactivation. In agreement with the inactivation-voltage relations (Fig. 2 C) there is a faster rate and greater relative amount of inactivation at 0 mV than at more positive potentials. Full-length Kv1.5 channels do not exhibit such a voltage dependence, and mean data are summarized in Table I. Here, inactivation of full-length Kv1.5 and Kv1.5ΔN209 during 20-s depolarizations have been fit to a biexponential decay function with fast (τ_1) and slow (τ_2) time constants. The difference between inactivation rates in the two channels is explained at 0 mV by the almost twofold faster rate of τ_2 in Kv1.5ΔN209 than in Kv1.5.

A second consequence of inactivation from late closed states is the observation of excessive cumulative inactivation, where more complete inactivation is observed when channels are repeatedly shuttled between positive and negative potentials. This allows channels to repeatedly pass through closed states, and results in more complete inactivation than would be observed if channels were held continuously in the open state. We have tested

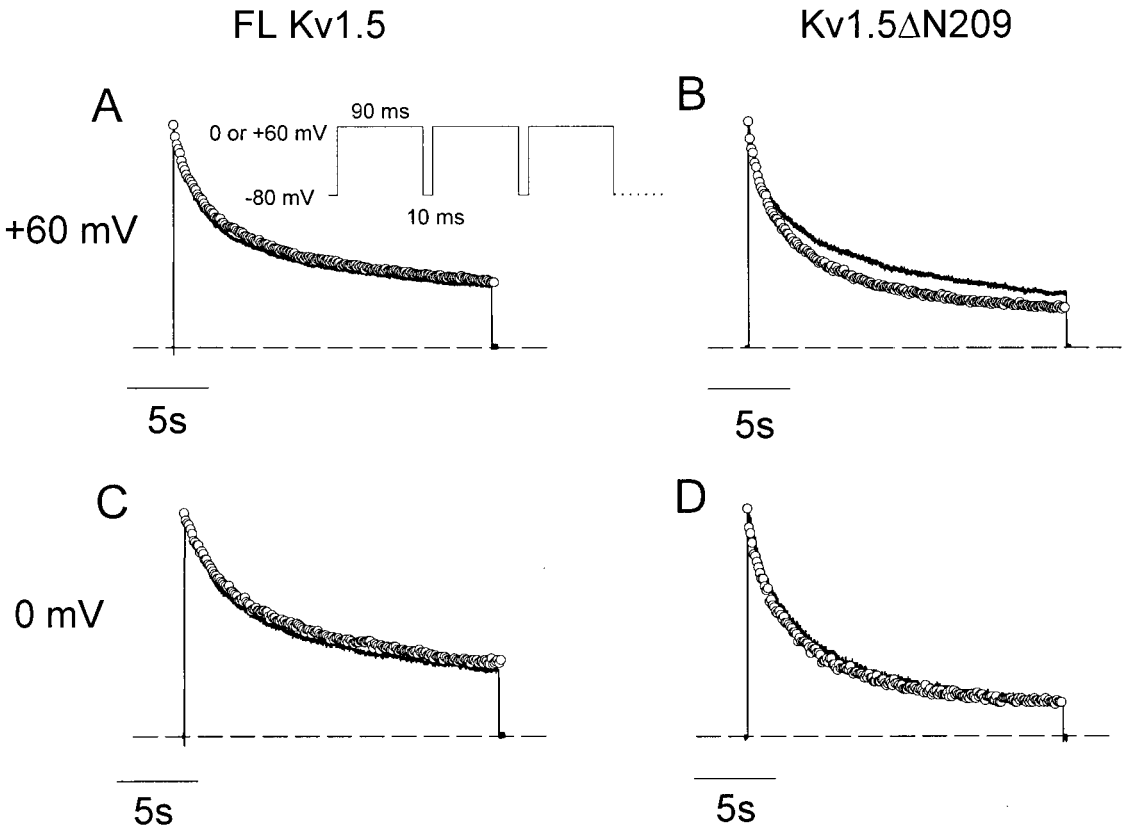

FIGURE 4. Excessive cumulative inactivation in Kv1.5 ΔN209. Cells expressing full-length (FL) Kv1.5 (A and C) or Kv1.5ΔN209 (B and D) were subjected to a 20-s depolarizing pulse to either 0 or + 60 mV (continuous traces in all panels). Subsequently, cells were subjected to a train of 200 pulses, each 90 ms in duration to either 0 or + 60 mV, and interspersed by 10-ms repolarizations to −80 mV. Normalized peak currents of the repetitive depolarizing pulses are plotted as open circles in each panel. Similar results were observed in six cells.

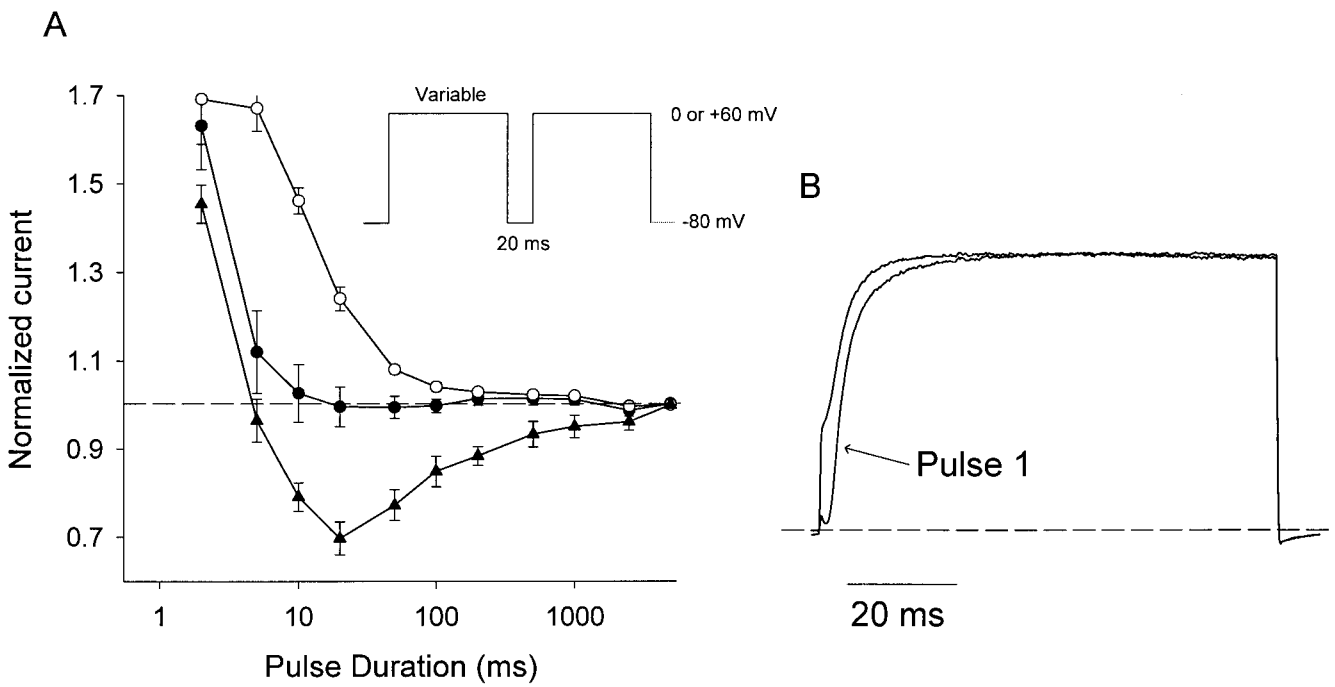

FIGURE 5. Excessive cumulative inactivation in Kv1.5ΔN209 depends on pulse duration. (A) A series of repetitive depolarizations to either 0 (open symbols) or +60 mV (closed symbols) was applied to HEK 293 cells expressing full-length (FL) Kv1.5 (○, ●) or Kv1.5ΔN209 (▲). Pulses were interspersed by 20- ms repolarizations to −80 mV, but the number of pulses and their duration were varied to generate a total depolarization time of 5 s. The residual current after each pulse train was normalized to the current remaining after a continuous 5-s pulse. (B) Representative currents from Kv1.5ΔN209 during 90-ms pulses to +60 mV. The currents during the first and second pulses of the train are illustrated and the second current shows the rapid rising phase of currents at this interpulse interval.

for excessive cumulative inactivation in full-length Kv1.5 and Kv1.5ΔN209, to ascertain whether closed state inactivation in the ΔN209 short form may explain the U-shaped inactivation-voltage relation. Representative records are shown in Fig. 4, in which cells were repetitively pulsed to a test potential (+60 or 0 mV) for 90 ms followed by a 10-ms repolarization period at −80 mV. The peak currents during each test pulse were compiled and their decay (shown as the open symbols) compared with the current decay observed during a continuous pulse to the test potential (solid line). Clearly, in Kv1.5ΔN209, rapid shuttling with a 90:10 duty ratio between 60 and −80 mV (Fig. 4 B) results in excessive cumulative inactivation, in that the peak current measured during the repetitive pulses falls below the current level during the continuous pulse at +60 mV. It is of note that shuttling the potential between 0 and −80 mV does not lead to excessive inactivation (Fig. 4 D), which is consistent with this potential being close to the minimum of the inactivation-voltage relationship (Fig. 2 C). Full-length Kv1.5, in contrast, exhibits no excessive cumulative inactivation under either condition.

To further characterize excessive cumulative inactivation in this channel, cells expressing full-length Kv1.5 or Kv1.5ΔN209 were subjected to repetitive depolarizations (−80 mV to 0 or +60 mV) in which the interpulse interval was held constant at 20 ms, but the pulse duration and number of pulses were varied such that the total depolarization time was 5 s (Fig. 5 A). The residual current observed after each pulse train was normalized to the current remaining at the end of a continuous 5-s pulse. In full-length channels, data denoted by the closed circles indicates that the amount of inactivation during a train of repetitive depolarizations from −80 to +60 mV never significantly exceeds the amount of inactivation that occurs during a continuous pulse (i.e., normalized current doesn't fall below 1.0). This observation is consistent with the assertion that the amount of inactivation observed is related to the total time spent depolarized, implying that in full-length Kv1.5, inactivation occurs primarily from the open state. Also, when pulsed repetitively between −80 and 0 mV, the relationship was shifted to longer pulse durations (open circles) than for the pulse trains between −80 and +60 mV. This observation is most likely due to the slower activation kinetics at 0 mV relative to +60 mV (Fig. 1), and again supports the idea that closed-state inactivation does not contribute substantially to full-length Kv1.5 inactivation, since channels would be expected to remain significantly longer in closed states when pulsed to 0 mV than when pulsed to +60 mV.

When the same protocol was applied to Kv1.5ΔN209, pulse trains to +60 mV with intermediate pulse durations (10–200 ms) resulted in substantially more inactiva-

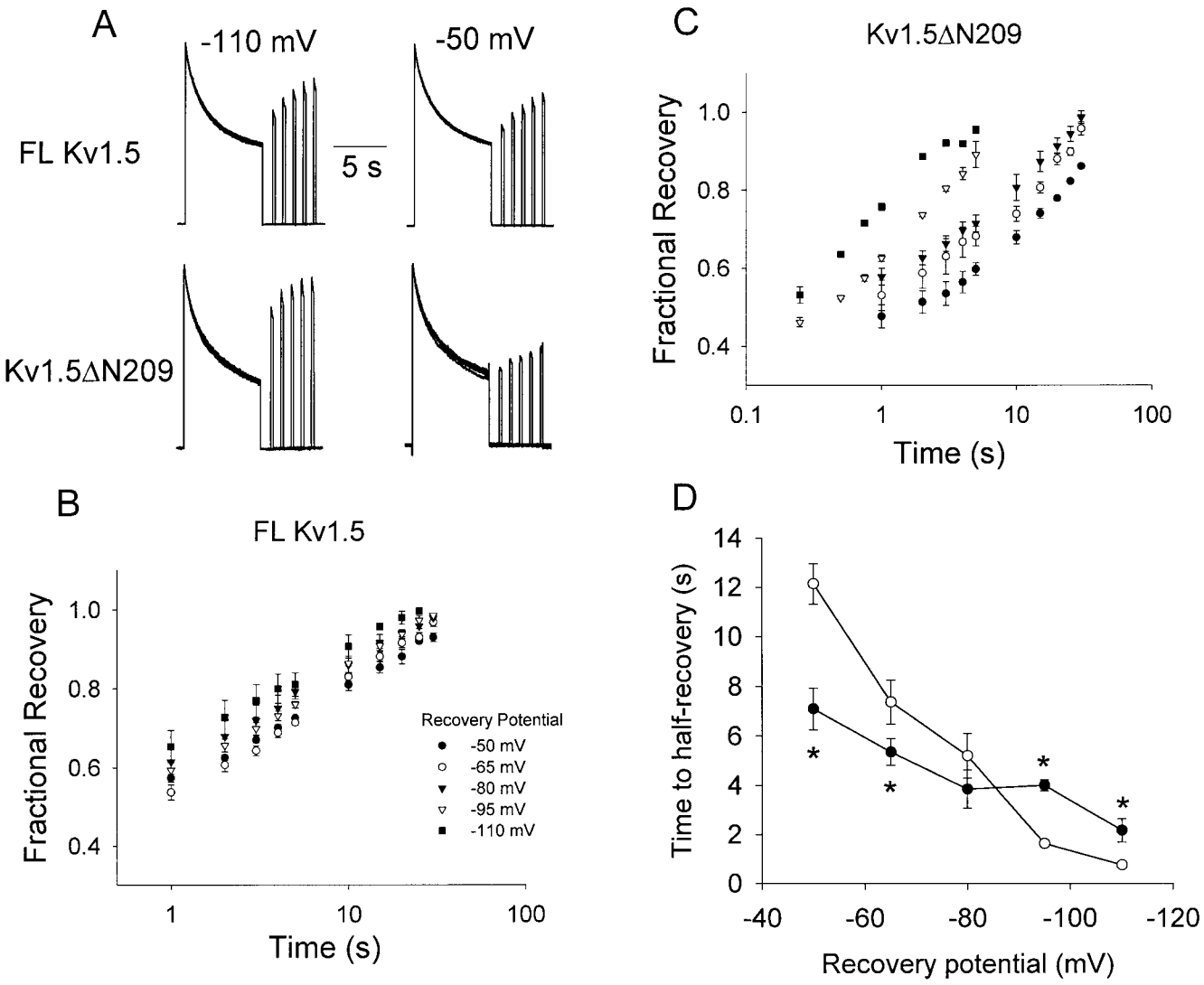

FIGURE 6. Voltage dependence of recovery from inactivation. (A) Cells expressing full-length (FL) Kv1.5 or Kv1.5ΔN209 were subjected to 7-s inactivating pulses at 60 mV, and tracings show recovery from inactivation at −110 and −50 mV. (B and C) Recovery in Kv1.5ΔN209 and full-length Kv1.5 was measured during 250-ms test pulses to +60 mV, after holding at recovery potentials between −50 and −110 mV for 0.25–30 s. (D) Time to half-recovery for full-length Kv1.5 (○) and Kv1.5ΔN209 (●) were determined at various recovery potentials by measuring the time required for current to reach the 50% recovery level.

tion than a continuous 5-s pulse. This finding suggests that the amount of inactivation observed is related to the number of times a channel shuttles between open and closed states. In simple terms, a high pulse frequency passes channels through closed states more often, and results in a greater amount of inactivation. This experiment suggests a marked shift in the state dependence of inactivation in the short form of Kv1.5, as inactivation in Kv1.5ΔN209 appears to occur from closed states, with or without a component of inactivation from the open state. An examination of individual data tracings during the 80-ms depolarizations in Kv1.5ΔN209 shows that, after the first pulse, currents rise extremely rapidly in all subsequent pulses (Fig. 5 B). The instantaneous rising phase of the second pulse current in Fig. 5 B is a driving force effect on the fraction of channels that have failed to close, however, there is also a reduction in the delay preceding channel opening, which indicates that channels lack the time to completely deactivate during the interpulse interval, and only reach early closed states in the deactivation pathway. Kv1.5 and Kv1.5ΔN209 channels deactivate with similar kinetics, and with deactivation time constants of roughly 6 ms at −80 mV one would expect slightly more than half of the channels to close during a 10-ms repolarizing pulse, which corresponds to the magnitude of the instantaneous current component relative to the total current activated (Fig. 5 B). If channels are inactivating from closed states, this observation suggests that these closed states are late in the activation pathway, very near to the open state.

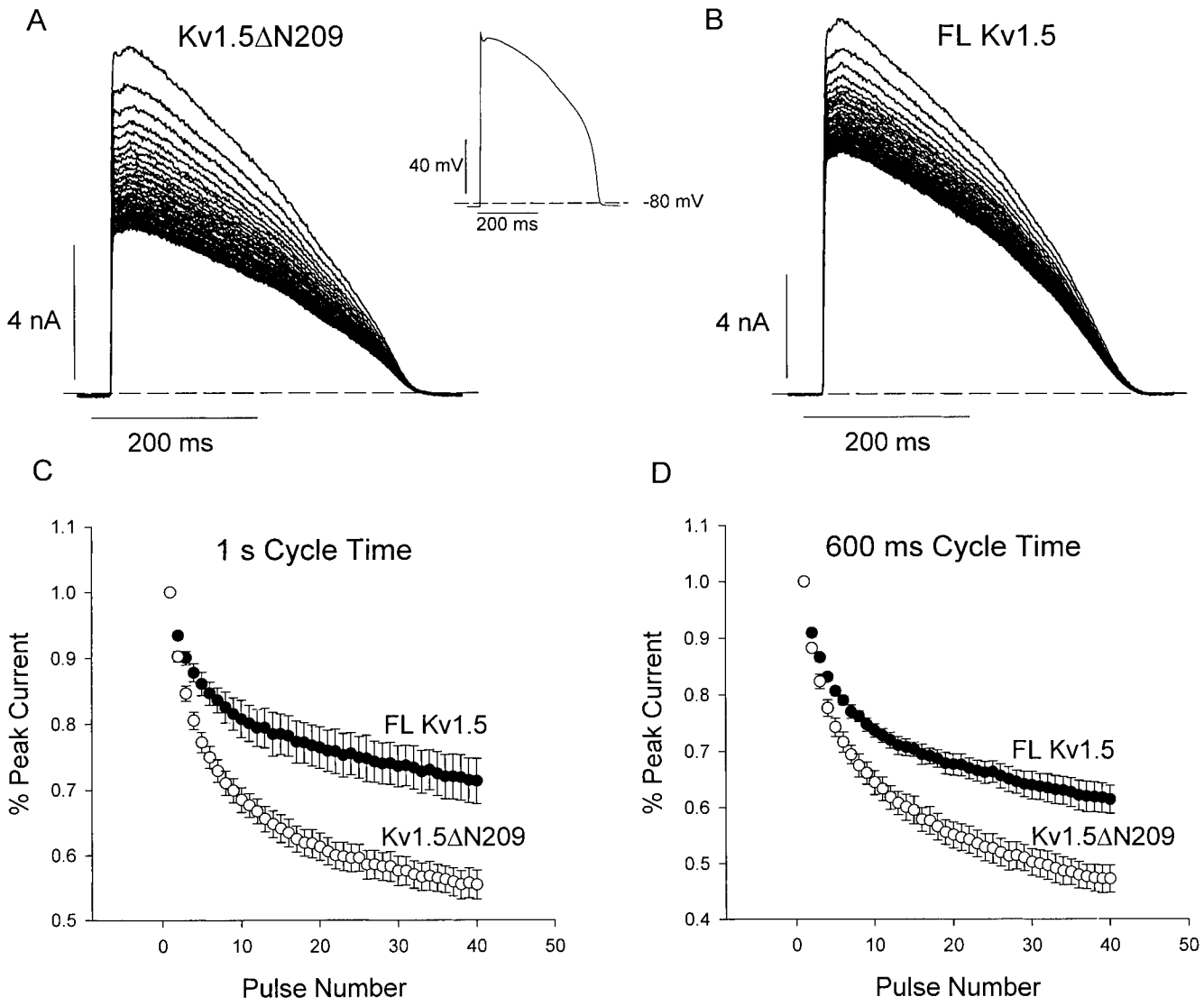

FIGURE 7. Excessive cumulative inactivation in Kv1.5ΔN209 using human action potential clamp. A human ventricular cardiac action potential was recorded during stimulation at 1 Hz as shown in the inset in A. This waveform was then used as the stimulus waveform to voltage clamp HEK 293 cells expressing Kv1.5ΔN209 (A) or full-length (FL) Kv1.5 (B). Currents are shown to decrease in both cases during constant stimulation from rest at 1 Hz. The peak currents during each pulse have been plotted in C and D for stimulation at 1Hz and at 1.7 Hz, respectively. In both cases, a significantly greater decrease in Kv1.5ΔN209 current was observed. Data are means of five to eight cells.

Recovery from Inactivation

We also observed that the voltage dependence of recovery from inactivation is markedly altered in Kv1.5ΔN209 channels (Fig. 6). HEK 293 cells expressing full-length Kv1.5 or Kv1.5ΔN209 were subjected to 7-s inactivating pulses at +60 mV, and the recovery at holding potentials between −50 and −110 mV was observed for up to 30 s. The difference in the voltage dependence of recovery is immediately evident upon examination of the representative traces presented in Fig. 6 A. In Kv1.5ΔN209, recovery is nearly complete within 2 s at −110 mV, but is extremely slow with a holding potential of −50 mV. In full-length Kv1.5, the time course of recovery appears to vary far less over the same voltage range. Summary data are shown for a range of recovery potentials between −50 and −110 mV for full-length Kv1.5 in Fig. 6 B, and Kv1.5ΔN209 in Fig. 6 C. The holding potential has a fairly minor effect on recovery from inactivation in full-length Kv1.5. However, in Kv1.5ΔN209, recovery from inactivation exhibits a much stronger voltage dependence. Overall, the half-time for current recovery in Kv1.5ΔN209 was found to vary roughly 20-fold over the voltage range examined, whereas recovery of full-length Kv1.5 was found to vary only approximately threefold. This difference was found to be significant at potentials of −50, −65, −95, and −110 mV (Fig. 6 D, $P < 0.05$).

Excessive Inactivation of Kv1.5ΔN209 under Cardiac Action Potential Clamp

To compare cumulative inactivation in full-length Kv1.5 and Kv1.5ΔN209 using a more physiological stimulus, we recorded an action potential from a human ventricular myocyte (at 1 Hz) and subjected transfected HEK 293 cells to this waveform repetitively at frequencies of either 1 or 1.67 Hz. The waveform is shown in the inset to Fig. 7 A. In both channels, inactivation accumulates over the course of the pulse trains, seen as a progressive decrease in the peak current during trains of action potential clamps (Fig. 7, A and B). Peak current during each pulse has been normalized to the current during the first pulse and plotted against the respective pulse number to illustrate the relative current decays over time at the two pulsing frequencies (Fig. 7, C and D). At both pulse rates, peak currents decrease substantially more in Kv1.5ΔN209 than in full-length Kv1.5, which suggests that in the physiological setting of the human heart, inactivation is likely to accumulate to a greater degree in Kv1.5ΔN209 than in the long form of the channel.

Kinetic Models of Inactivation Models Predicting U-shaped Inactivation-voltage Relationships

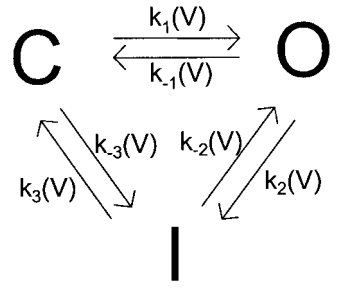

(SCHEME I)

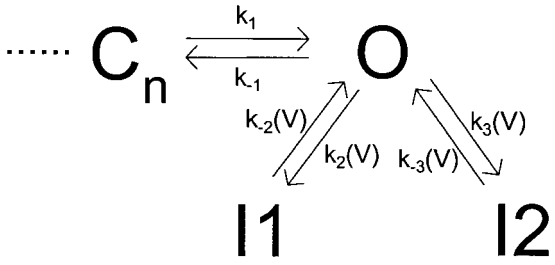

(SCHEME II)

Apart from the Ca^{2+} current–dependent inactivation of L-type Ca^{2+} channels, models that predict a U-shaped inactivation-voltage relationship can be divided into two classes. The first of these is characterized by voltage-dependent microscopic inactivation rates between the open state and one or more inactivated states (Schemes I and II). An example is the three-state cyclic model of Jones and Marks (1989; Scheme I), formulated to describe the U-shaped inactivation-voltage relationship of Ca^{2+}-currents in bullfrog sympathetic neurons. The primary feature of these models are that the microscopic inactivation rates are voltage-dependent, which itself confers a voltage dependence to inactivation, or causes disparate entry into one or more inactivated states. Clearly, the model structures in Schemes I and II require the postulation of some intrinsic voltage-sensor for inactivation.

The second class of model describing a U-shaped inactivation-voltage relationship is characterized by accelerated inactivation from an intermediate state in the activation pathway. Examples include the model of Klemic et al. (1998) describing the inactivation of Kv2.1, and the model of Patil et al. (1998) for inactivation of N-type Ca^{2+} channels. In this class of model, the voltage dependence of microscopic deactivation and (in some models) microscopic activation results in enhanced occupancy of rapidly inactivating intermediate states with moderate depolarizations and, hence, an accelerated time course of inactivation at these intermediate potentials. Importantly, the second class of model is unique among published models in its prediction of excessive cumulative inactivation. The first class of model fails to predict excessive cumulative inactivation without substantial acceleration of inactivation from closed states. Finally, the second class of model does not require the postulation of a voltage sensor for inactivation, which is significant as the full-length Kv1.5 channel does not exhibit a voltage-dependent inactivation process.

We considered two specific models in this second class, as shown in Schemes III and IV. In Scheme III, the channel is proposed to occupy multiple open states in a voltage-dependent manner, with inactivation occurring most readily from the first open state; i.e., k_3, k_4, and k_5 are voltage-independent transitions, but k_4 is $> k_5$. If depolarization favors occupancy of the second open state, the model predicts a U-shaped voltage dependence of inactivation, and excessive cumulative inactivation, because strongly depolarized channels will repeatedly pass through the first open state during trains of repetitive depolarizations, giving them an increased likelihood of inactivating. However, the model does not predict a dissociation of the voltage dependencies of activation from inactivation as we observed in Kv1.5ΔN209.

In Scheme IV (Fig. 8), the model structure parallels that of Scheme III, but the model contains a single open state. Voltage-dependent microscopic activation and deactivation rates predict greater occupancy of a late closed-state at intermediate potentials. If $k_3 > k_2$, the model predicts more rapid inactivation at intermediate potentials. This model also predicts excessive cumulative inactivation, as channels will repeatedly pass through the late closed state during repetitive depolarizations. In the con-

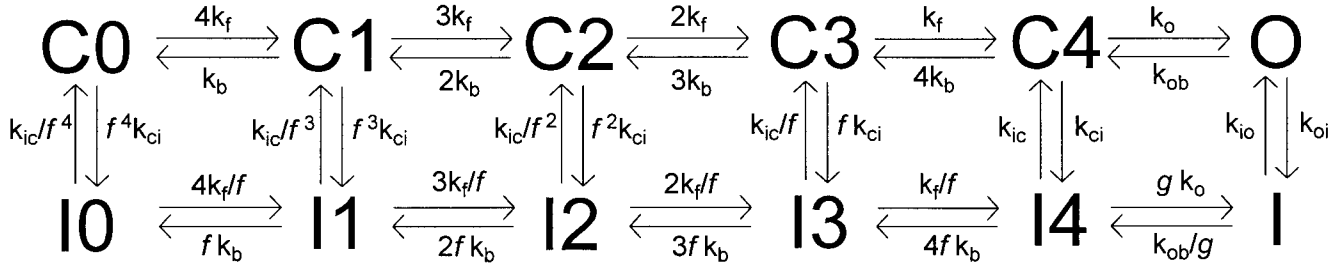

FIGURE 8. Schematic representation of inactivation in full-length Kv1.5 and Kv1.5ΔN209. The rate constants in the activation pathway (horizontal transitions) were governed by exponential functions of voltage (see MATERIALS AND METHODS). The factor g was defined as $\sqrt{[(k_{oi} \cdot k_{ic})/(k_{io} \cdot k_{ci})]}$. At 0 mV, the rate constants were (in ms^{-1}) $k_f = 0.4$, $k_b = 0.065$, $k_o = 0.31$, and $k_{ob} = 0.017$, with associated valences of $z = 1.4$ for k_f, $z = 0.35$ for k_b, $z = 0.38$ for k_o and $z = 0.70$ for k_{ob}. Vertical transitions were voltage-independent. Rate constants of vertical transitions for simulation of full-length Kv1.5 were (ms^{-1}) $k_{ci} = 0.00008$, $k_{ic} = 0.000055$, $k_{oi} = 0.00017$, and $k_{io} = 0.000061$, $g = 1.39$, and the allosteric factor f was 0.64. For simulations of Kv1.5ΔN209, parameters were (ms^{-1}) $k_{ci} = 0.0013$, $k_{ic} = 0.0000054$, $k_{oi} = 0.00017$, and $k_{io} = 0.000061$, $g = 0.11$, and the allosteric factor f was 0.3.

text of Scheme IV, we would hypothesize that deletion of the NH_2 terminus of Kv1.5 causes accelerated inactivation from late closed states, similar to the model proposed for inactivation of Kv2.1. The model of Klemic et al. (1998) is of this form and, as shown in Fig. 8, proposes allosteric coupling of closed-state inactivation to transitions along the activation pathway as a mechanism to account for accelerated inactivation from late closed states. It is a particularly attractive way to describe our results, as this model predicts a strong voltage dependence of recovery from inactivation, in addition to a U-shaped inactivation-voltage relationship and excessive cumulative inactivation, as was observed in Kv1.5ΔN209. As well, it is in agreement with a single open state for *Shaker* channels (Hoshi et al., 1994).

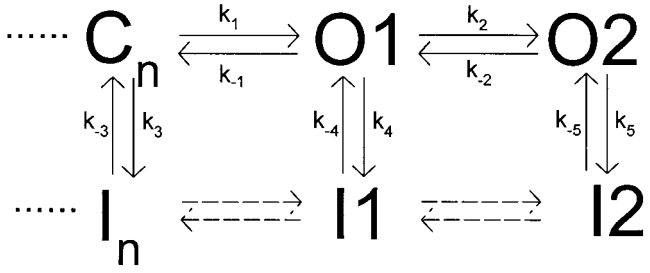

(SCHEME III)

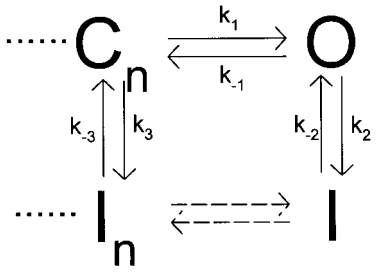

(SCHEME IV)

Building a Kinetic Model of Inactivation in Kv1.5 and Kv1.5ΔN209

With the above considerations in mind, we constructed a model based upon the previously published model of Kv2.1 inactivation. The model consists of 12 states: five closed states, five closed-inactivated states, one open state, and one inactivated state (Fig. 8). Horizontal transitions between states are governed by exponential functions of voltage, and the model assumes four independent transitions along the activation pathway. Vertical transitions were assumed to be independent of voltage. Forward (k_o) and backward (k_{ob}) rates between the open state and final closed state were governed by exponential functions of voltage, and were determined by fitting the voltage dependence of time constants of single exponential fits of deactivation and activation rates (data not shown). The resulting activation transitions reproduce the experimentally observed kinetics and voltage dependence of activation in the full-length channel (Fig. 9 A), with simulations yielding a $V_{1/2}$ of activation of −12 mV. Also, current records from long 20-s pulses to +60 mV in the full-length channel were used to estimate the forward and backward rates of inactivation from the open state (k_{oi}, k_{io}), based on the assumption that most inactivation was occurring from the open state in the full-length channel. The parameter g is included to preserve microscopic reversibility. We then systematically varied the rates of inactivation from the open state and closed states, to investigate the potential influence of closed-state inactivation in the different forms of Kv.1.5.

We found that the rate of inactivation from the open state was the prime determinant of the time course of inactivation at depolarized potentials. This is expected, due to the strong bias toward the open state with strong depolarizations predicted by our activation parameters (Fig. 9 B). Our simulations predict that above 10 mV, >90% of channels occupy the open state (Fig. 9 B). In

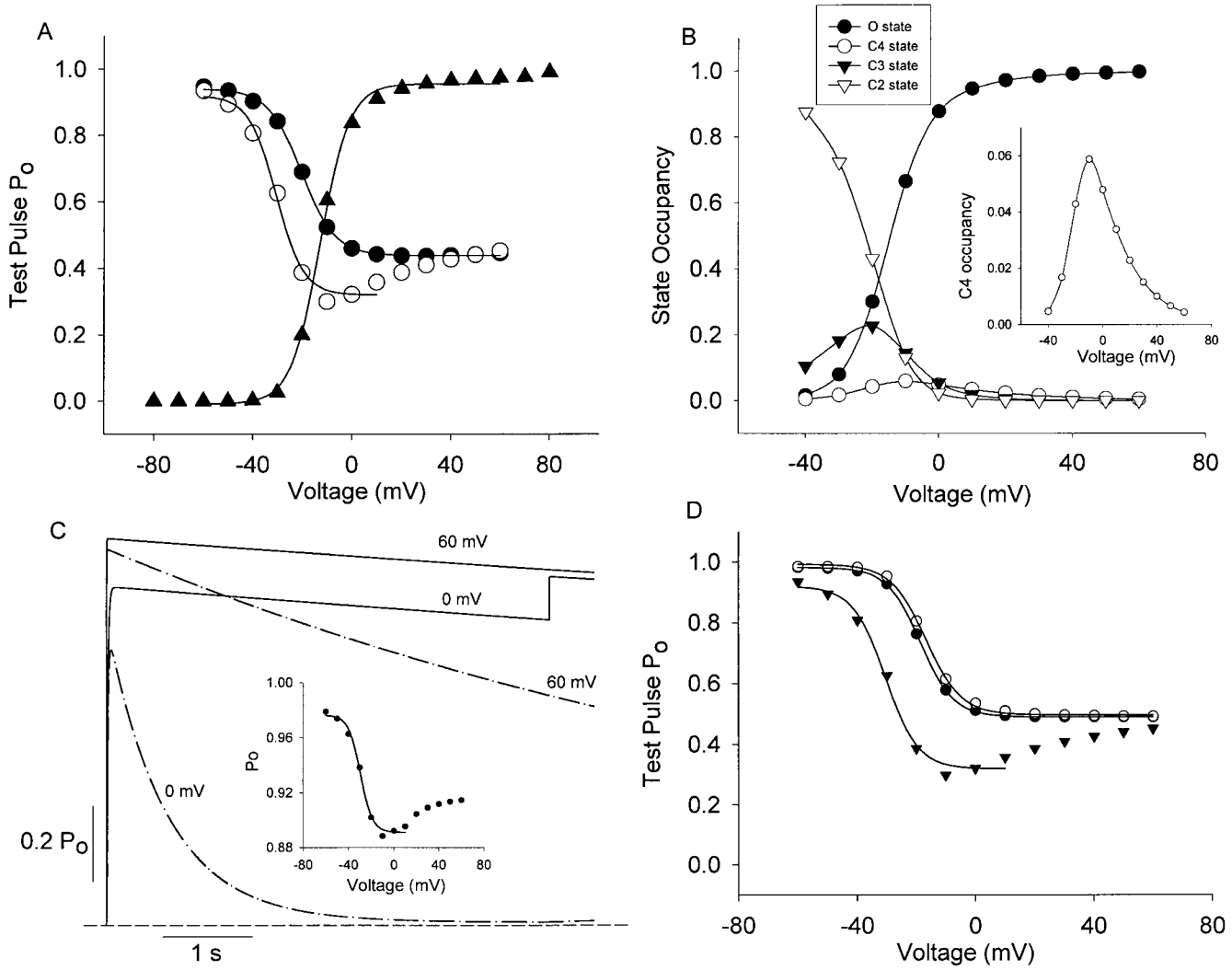

FIGURE 9. Simulated effects of alterations to closed and open-state inactivation rates. (A) Activation relationship (▲) and inactivation-voltage relationships simulated for full-length (FL) Kv1.5 (○) and Kv1.5ΔN209 (●), using the parameters presented in Fig. 8. The activation relationship was generated using the protocol described in Fig. 1. Inactivation-voltage relationships were generated using the protocols described in Fig. 2 C. (B) Predicted voltage-dependent state occupancy in full-length Kv1.5 and Kv1.5ΔN209, measured after brief (60 ms) simulated depolarizations to each potential, with parameters from Fig. 8. In C and D, k_{ic} was set to 0.0000054 ms^{-1}, f was set to 0.3, and k_{ci} was altered as noted. (C) Simulated currents after deceleration of inactivation from the open state (k_{oi} in Fig. 8) to 0.000017 ms^{-1} (solid lines) exhibit extremely slow inactivation, but result in a U-shaped inactivation-voltage relationship (inset). Acceleration of k_{ci} (Fig. 8) to 0.02 ms^{-1} (dotted lines) results in more accurate reproduction of inactivation at +60 mV, but extremely exaggerated inactivation at 0 mV. (D) Alterations of the closed state inactivation rates shift the inactivation $V_{1/2}$. Steady-state inactivation relationships were simulated using the protocol described in Fig. 2 C, with k_{ci} rates of 0.000000017 (●), 0.00008 (○), and 0.0013 (▲) (Fig. 8) yielding inactivation $V_{1/2}$s of −17, −19, and −29 mV, respectively.

the formulation of the model presented in Fig. 8, simulations of the inactivation-voltage relations resulted in behavior qualitatively resembling the full-length channel, as long as the closed-state inactivation rate was roughly equal to or less than the rate of open-state inactivation. However, the model produces essentially monoexponential kinetics of inactivation, in contrast to the biexponential kinetics observed experimentally. The only noted alteration of the inactivation-voltage relationship upon deceleration of the closed-state inactivation rate is a depolarizing shift of the $V_{1/2}$ of inactivation (Fig. 9 D). To adequately describe the dissociation between the half-activation and half-inactivation potential (roughly an 8-mV hyperpolarizing shift) in full-length Kv1.5, we estimated a closed-state inactivation rate of 0.00008 ms^{-1} (k_{ci}; Fig. 8). The inactivation-voltage relationship derived from this simulation (Fig. 9 A) was fit with a Boltzmann function to yield a $V_{1/2}$ of −20 mV, which is close to the value observed experimentally in the full-length channel.

Incorporating the U-shaped Voltage Dependence

A number of possible changes to the model can result in a U-shaped inactivation-voltage relationship. Initially, we examined the effects of destabilization of inactivation from

the open state. Deceleration of the rate of open-state inactivation not only results in a U-shaped inactivation-voltage relationship (Fig. 9 C, inset), but also results in very slow inactivation that poorly reproduces the time course of inactivation observed at depolarized potentials (Fig. 9 C, solid lines). In addition, a far more significant acceleration of closed-state inactivation is required to approximate the time course of inactivation experimentally observed with strong depolarizations. For example, deceleration of inactivation from the open state by 10-fold (chosen because it is sufficient to generate a mildly U-shaped inactivation-voltage relationship) requires acceleration of closed-state inactivation by roughly 250-fold to reproduce the experimentally observed time course of inactivation at +60 mV (Fig. 9 C, broken lines). The result of such an acceleration is more profound inactivation at intermediate potentials—in our example, we see complete inactivation within 2.5 s at 0 mV (Fig. 9 C)–and consequently an exaggerated U-shape of the inactivation-voltage relationship.

A second kinetic change that could account for a U-shaped inactivation-voltage relationship is simply acceleration of inactivation from closed states. This possibility was particularly attractive, thanks to unique insights gained through comparisons of the ΔN209 channel with the full-length channel. As noted, inactivation of Kv1.5ΔN209 was more complete than for full-length Kv1.5 at intermediate potentials, but gradually approached the level observed in the full-length channel at more positive potentials. This can be explained by the presence or enhancement of an inactivation mechanism in addition to the primarily open-state inactivation observed in full-length Kv1.5. More importantly, deeper inactivation at intermediate voltages in Kv1.5ΔN209 is a rigid prediction of the model, and is not necessarily predicted by a model based on destabilization of inactivation from the open state.

Acceleration of inactivation transitions from closed-states of the channel results in a gradual leftward shift of the inactivation-voltage relationship, without affecting the activation relationship, and further acceleration results in a U-shaped steady-state inactivation relationship (Fig. 9 D). Acceleration of closed-state inactivation to 0.0013 ms^{-1} results in a 17-mV dissociation between half-activation and half-inactivation potentials, and a marked U-shaped inactivation-voltage relationship (Fig. 9 A; it is important to note that we have not considered the 10-mV hyperpolarizing activation shift in Kv1.5ΔN209, and hence the $V_{1/2}$ of the Boltzmann fit in Fig. 9 D reproduces the enhanced dissociation of inactivation from activation, but not the true half-inactivation potential in Kv1.5ΔN209).

Excessive Cumulative Inactivation

The parameters derived using the approach described above also allowed effective simulation of excessive cumulative inactivation in full-length Kv1.5 and Kv1.5ΔN209. Simulations of the repetitive 90-ms depolarizations (+60 mV) and 10-ms repolarizations (−80 mV) described in Fig. 4 are shown in Fig. 10 A. Clearly, the parameters derived for the full-length channel predict little or no excessive cumulative inactivation. In contrast, the parameters derived for Kv1.5ΔN209 predict excessive cumulative inactivation that is maintained throughout the 20-s pulse train with the absence of any crossover, as observed experimentally.

The allosteric factor, *f*, reflects the extent to which inactivation is favored in partially activated states of the channel (Fig. 8). It affects the half-inactivation voltage, since *f* governs the relative rates of inactivation and recovery at potentials where few or no channels reach the open state. For the same reason, *f* also exerts a very obvious effect on the voltage dependence of recovery from inactivation. Having roughly determined the rates of inactivation from late closed states, we used the rates of recovery at extremely negative potentials (i.e., −110 mV; Fig. 6) to fix a rate for recovery from the earliest closed state. This line of reasoning was based on the assumption that extremely hyperpolarized recovery potentials would result in the vast majority of channels dwelling in their earliest closed state, and is corroborated by our observation of a single-exponential recovery time course at hyperpolarized recovery potentials. Finally, the allosteric factor *f* can be fixed by studying its effects on the predicted voltage dependence of recovery.

This approach can be used to adequately fit the voltage dependence of recovery in both full-length Kv1.5 and Kv1.5ΔN209, however, it does not predict the crossover of their respective recovery rates at −80 mV, as was observed experimentally (Fig. 6). To reproduce this feature of our experimental data, slight changes must be made to the modeled rates of recovery from inactivation (compare k_{ic} for the long and short forms of Kv1.5 in legend for Fig. 8, and simulations shown in Fig. 10, B and C). Finally, although this model predicts a strong voltage dependence of recovery in Kv1.5ΔN209 (Fig. 10, B and C), it does not identically reproduce the voltage dependence of recovery observed experimentally (Fig. 10 C and Fig. 6, B and C). Most likely, this difficulty arises because of our simplification of the Kv1.5 activation pathway, as the model implies that the voltage-dependent occupancy of different closed-states governs the voltage dependence of the recovery pathway.

It is widely held that the steps involved in Kv1 channel activation are far more complex than those depicted here (Zagotta et al., 1994a,b; Schoppa and Sigworth, 1998). Although the model generates reasonably accurate reproductions of the activation relationships and activation kinetics of Kv1.5 (Fig. 9 A), it is not intended to provide a quantitative description of the activation pathway in Kv1.5 in all details.

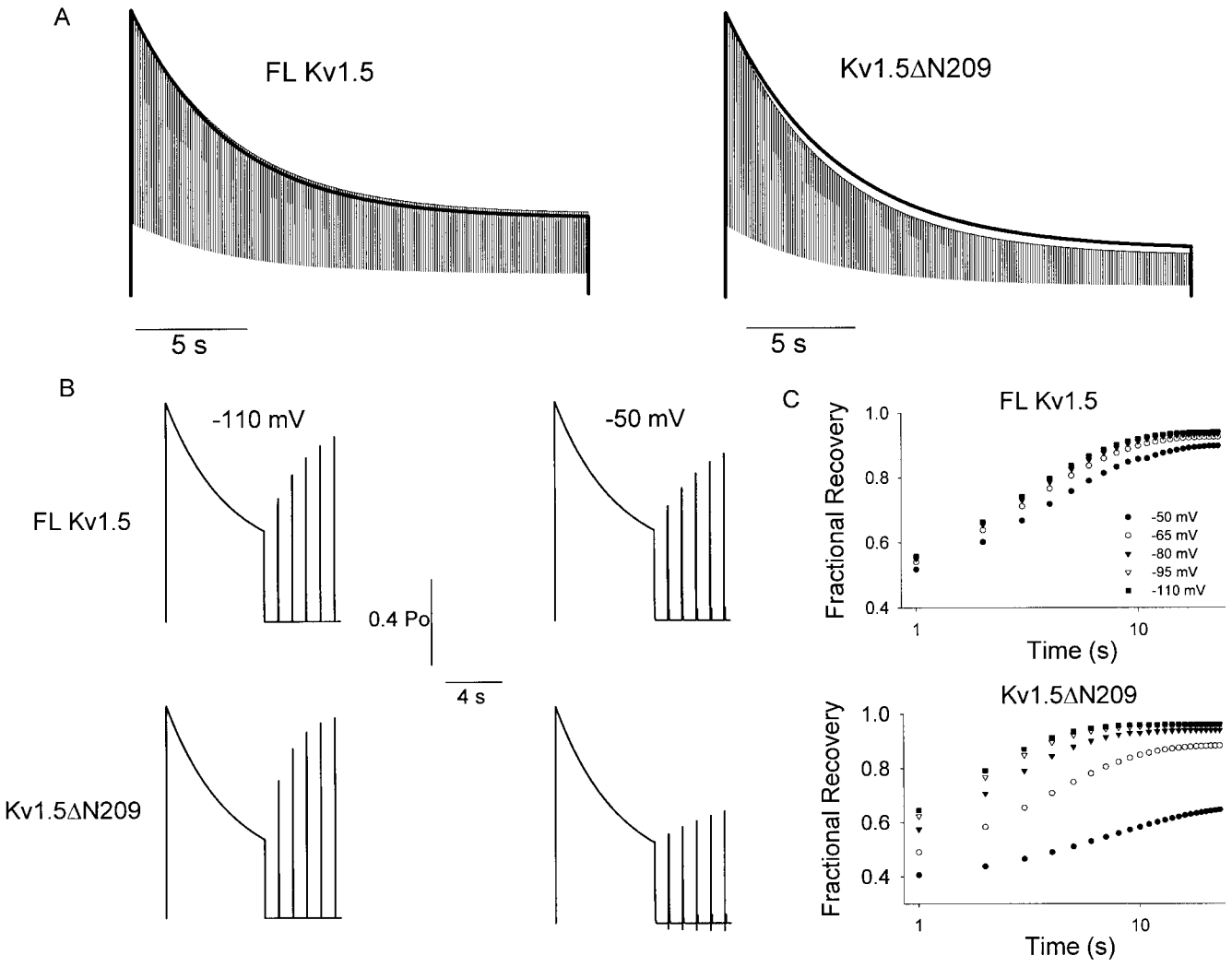

FIGURE 10. Simulations generated from the kinetic model of inactivation in Kv1.5ΔN209 and full-length Kv1.5. (A) Simulated excessive cumulative inactivation in full-length (FL) Kv1.5 and Kv1.5ΔN209. Currents were simulated with a 20-s continuous depolarizing pulse to +60 mV (heavy line) or with a 20-s train of 90-ms depolarizations to +60 mV separated by repolarizations to −80 mV. (B) Voltage-dependent recovery from inactivation in full-length Kv1.5 and Kv1.5ΔN209. Currents were simulated with a 7-s depolarizing pulse to +60 mV, followed by recovery at −110 or −50 mV for up to 5 s. (C) The time course of recovery in full-length Kv1.5 and Kv1.5ΔN209 was simulated at −50,−65, −80, −95, and −110 mV, with test pulses at 1-s intervals after a 7-s depolarizing pulse to +60 mV.

DISCUSSION

A Change in the State Dependence of Inactivation in the Short Form of Human Kv1.5

We have shown that the activation, inactivation, and recovery properties of Kv1.5ΔN209 are significantly modified from those of the long form, or full-length Kv1.5. Activation is affected only in a minor way, with a small, but significant, hyperpolarizing shift in the half-activation potential, and a decrease in the slope (Fig. 1). The ΔN209 short form of Kv1.5 lacks almost the entire cytoplasmic NH_2-terminal domain and a significant portion of the T1 intersubunit assembly domains, including all of T1A and most of the T1B portion (Shen and Pfaffinger, 1995). The small changes in channel steady-state activation properties are consistent with those that have been described for an extensive ΔT1 *Shaker* mutant (Kobertz and Miller, 1999), although we found that current activation rate was mildly accelerated in the truncated form, instead of slowed. The most important changes that we have observed in the kinetic properties of the short form of Kv1.5 are related to the nature of C-type inactivation in this channel. Kobertz and Miller (1999) found that N-type inactivation was relatively unaffected by T1 deletion, but Kv1.5 does not possess the machinery for this type of rapid inactivation and exhibits a slower, pore-dependent inactivation.

The striking observation that we have made here is that the short form of Kv1.5 shows a marked shift in the state dependence of its inactivation from that found in the full-length channel. Our experimental data show that inactivation in full-length Kv1.5, as in most voltage-

gated K^+ channels, increases with voltage and eventually stabilizes, so that the inactivation-voltage relationship reaches a basal level at depolarized potentials. In Kv1.5, for very long pulses this is at ~40% of the maximum current (Fedida et al., 1999); although, it should be noted that inactivation can be almost complete when Na^+ permeates the channel (Wang et al., 2000). In Kv1.5ΔN209, inactivation shows a prominent upturn when studied in both HEK 293cells and mouse L cells (Fig. 2), a property that has only been described before in WT Kv2.1 channels and its heteromultimers (Klemic et al., 1998; Kramer et al., 1998; Kerschensteiner and Stocker, 1999). This was ascribed to inactivation from closed states allosterically coupled to voltage sensor movement with little inactivation from the open state. The characteristics of this kind of inactivation were a voltage-dependent recovery from inactivation and the phenomenon of excessive cumulative inactivation. Wild-type Kv1.5 channels exhibit neither voltage dependence to inactivation (Fig. 3 A and Table I), nor do they show excessive cumulative inactivation at any potential (Figs. 4 and 5), and only mild voltage dependence to the recovery from inactivation (Fig. 6 B). In contrast, the studies we have performed on Kv1.5ΔN209 demonstrate a voltage dependence to its inactivation equivalent to that seen in Kv2.1 (Fig. 3 and Table I). Kv1.5ΔN209 also shows excessive cumulative inactivation (Figs. 4 and 5) and significant voltage-dependent recovery from inactivation (Fig. 6 C), although this is less marked than for Kv2.1 (Klemic et al., 1998). The upturn of the inactivation-voltage relationship is more correctly described as a more complete inactivation of Kv1.5ΔN209 at intermediate potentials with a nadir at around −20 or −10 mV, and a relief of inactivation at more positive potentials (Fig. 2). Finally, these altered properties of Kv1.5ΔN209 result in a marked increased in accumulation of inactivation during repetitive depolarizations using a human cardiac action potential as the stimulus waveform (Fig. 7).

Structural Basis for Closed State Inactivation in Kv1.5ΔN209

Our data suggests that the NH_2 terminus of Kv1.5 is involved in destabilizing the transition between the closed and closed-inactivated states of the channel. Several NH_2-terminal deletions and point mutations have been described that modulate activation gating kinetics and the voltage dependence of activation in *Shaker*, but none have characterized direct modulation of the slow inactivation gating of a *Shaker* homologue (Kobertz and Miller, 1999; Cushman et al., 2000; Minor et al., 2000). We have not examined whether the closed-state inactivation observed in Kv1.5ΔN209 occurs via classical C-type inactivation and, hence, can be modulated by pore occupancy. The current view of slow inactivation is that it involves conformational changes of the outer pore mouth, and recent studies suggest that interactions between residues in the S4 and S6 transmembrane segments are also critical in preventing closure of the slow inactivation gate until after channel opening (Loots and Isacoff, 2000).

Some preliminary studies in our laboratory have shown that the distal Kv1.5 NH_2 terminus (roughly the first 120 residues) is not required for the maintenance of normal inactivation gating, suggesting that residues within T1 are involved in the modulation of inactivation. The implied coupling of the NH_2 terminus to conformational changes in distal regions of the protein is interesting in light of recent reports postulating that the NH_2-terminal T1 tetramer hangs away from the inner mouth of the channel pore of *Shaker* channels (Gulbis et al., 2000; Kobertz et al., 2000; Zhou et al., 2001). There also have been reports of single molecule electron microscopy studies confirming this model (Kobertz et al., 2000). However, the structural basis for modulation of pore mechanics by the NH_2 terminus remains far from clear.

Model of Kv1.5ΔN209 Inactivation

Our comparison of full-length Kv1.5 and Kv1.5ΔN209 provided the important insight that the time course of inactivation is accelerated in Kv1.5ΔN209 at intermediate potentials, but slows and approaches that of full-length Kv1.5 at more extreme depolarizations. The simplest interpretation of this observation is that the ΔN209 deletion allows an additional avenue for inactivation, which is favored at intermediate potentials, and our kinetic model supports this hypothesis. In particular, we have shown that the inactivation-voltage relationship and excessive cumulative inactivation of Kv1.5ΔN209 can be reproduced by accelerating the rates of inactivation from closed-states of the channel, and allowing inactivation to proceed from the open state at rates observed in the full-length channel. The result of this model is that the truncated channel behaves similarly to full-length Kv1.5 at depolarized potentials, but inactivates more rapidly and completely (over the time intervals examined) at intermediate potentials where few channels are open. In addition, the acceleration of inactivation from closed-states predicts enhanced dissociation of inactivation from activation (Fig. 9, A and D). All of these features of the model are consistent with experimental data.

The most fundamental insight gained from our modeling is that the NH_2 terminus of Kv1.5 modulates the inactivation phenotype primarily by regulating the amount of inactivation that occurs from late closed-states. In addition, our model suggests that the mechanism for this acceleration is a shift in the allosteric coupling of inactivation to transitions through the activa-

tion pathway. Although the mechanism implied by our model is not the only possible way to accelerate closed-state inactivation, this mechanism is also consistent with our observation of enhanced voltage dependence of recovery in Kv1.5ΔN209. Furthermore, the concept of allosteric coupling of inactivation and/or recovery to transitions in the activation pathway is implied in a number of recent models of inactivation of voltage-gated K^+, Na^+ and Ca^{2+} channels (Kuo and Bean, 1993; Marom and Abbott, 1994; Olcese et al., 1997; Klemic et al., 1998).

Although the model structure is essentially identical to that of Klemic et al. (1998), it is important to notice that the model makes certain different predictions regarding state occupancy of the channel (Fig. 9 B). Most importantly, the model predicts that the bulk of inactivation occurs from the open state at depolarized potentials, primarily as a result of the extremely fast activation rates (Figs. 8, 9 C). This is an important departure from the model of Klemic et al. (1998) in which inactivation from the open state is extremely unfavorable. The rate of inactivation from the open state in Kv2.1 can be reduced 10,000-fold and substantial inactivation is still observed even at relatively extreme depolarizations, whereas deceleration of open-state inactivation by even 10-fold in our model for Kv1.5 results in nearly complete abolition of inactivation (Fig. 9 C). Furthermore, unlike Kv2.1, this model suggests that a substantial fraction of Kv1.5ΔN209 inactivation during repetitive depolarizations occurs from the open state of the channel, rather than late closed states. Inactivation from late closed states provides an additional inactivation mechanism that accounts for the deeper inactivation observed due to increased state occupancy at intermediate depolarizations or during repetitive pulse trains.

An important issue for consideration is why we observe relatively minor dissociation of activation from inactivation in Kv1.5ΔN209 in spite of the proposed rapid rates of closed-state inactivation. This is especially striking in comparison with Kv4.1 in which the half-activation and half-inactivation potentials are dissociated by as much as 40 mV (Jerng et al., 1999). However, our results are less different from Kv2.1, where the half-activation and half-inactivation potentials are dissociated by only 15 to 20 mV (VanDongen et al., 1990) in spite of the apparent involvement of closed-state inactivation (Klemic et al., 1998). It should be noted that a model of pure open-state inactivation can predict substantial dissociation of activation and inactivation as long as the inactivation rate far exceeds the recovery rate. However, far more rapid inactivation kinetics than those observed experimentally for Kv1.5 are required to simulate any significant dissociation from activation during the 5-s depolarizations used in our experiments (Fig. 2). Our simulations, and comparisons with recent models of Kv4 gating (Jerng et al., 1999) suggest that the primary reason for the relatively small dissociation of activation and inactivation is the strong bias toward opening in Kv1 channels. Kv4.1, in contrast to Kv2.1 and Kv1.5, has been recently modeled with deactivation rates three times faster than opening rates. The relatively concerted opening transition of Kv1 channels effectively reduces occupancy of late closed states, and prevents substantial closed-state inactivation.

Physiological Implications of Closed State Inactivation

Of particular interest in the present study is that NH_2-terminally truncated forms of Kv1.5 have been identified in murine and human cardiac myocytes that may arise from an unusual splicing mechanism within the Kv1.5 gene structure (Attali et al., 1993). The presence of the short form of Kv1.5 has been confirmed by Northern blot analysis, which revealed distinct bands of Kv1.5 RNA in mouse tissues and human heart (Tamkun et al., 1991; Attali et al., 1993; Fedida et al., 1993). Since there remains uncertainty with regards to the genotypes underlying the various K^+ currents in heart and vasculature, the altered phenotype of short forms of Kv1.5 suggests an important mechanism by which K^+ current diversity may be generated in many tissues.

We have not studied the effects of NH_2-terminal deletions of other Kv1 channels, although Kv1.1, 1.2, and 1.3 all possess alternative start sites homologous to M210 in Kv1.5. There have been a number of studies of NH_2-terminal deletions of *Shaker* and its Kv1 homologues, and none have reported any significant disruption of inactivation, so we suspect that these effects may be unique to Kv1.5. Since our data suggests that deletion of the NH_2 terminus affects the depth of inactivation, it seems likely that differential expression of this channel could alter the properties of outward K^+ currents in tissues such as cardiac muscle and vascular smooth muscle. For example, the expression of Kv1.5ΔN209 could increase the sensitivity of action potential duration to heart rate, as inactivation of Kv1.5ΔN209 is enhanced by repetitive depolarizations, and during action potential clamp experiments (Fig. 7). Also, maximal inactivation of Kv1.5ΔN209 occurs at potentials near the plateau of the cardiac action potential, so small physiological or pathophysiological changes in action potential shape could significantly affect inactivation of the channel. In addition, the T1 domain is required to maintain the specificity of subfamily subunit assembly, and the Kv1.5ΔN209 isoform will lack binding sites for both β subunits (Accili et al., 1997) and α-actinin-2 (Maruoka et al., 2000), as well as several phosphorylation sites within the NH_2 terminus. In particular, coupling to the actin cytoskeleton through α-actinin-2 has been implicated in modulating

the expression level of Kv1.5 (Maruoka et al., 2000). All these differences suggest that the short form of the channel may be subject to different regulation than the full-length Kv1.5 channels.

We thank Dr. Rolf Joho for his gift of Kv2.1, and Qin Wang for assistance in preparing the cells.

This study was supported by grants from the Heart and Stroke Foundations of British Columbia and Yukon, and the CIHR to D. Fedida. H. Kurata was supported by a University Graduate Fellowship from the University of British Columbia.

Submitted: 12 February 2001
Revised: 1 August 2001
Accepted: 2 August 2001

REFERENCES

Accili, E.A., J. Kiehn, Q. Yang, Z.G. Wang, A.M. Brown, and B.A. Wible. 1997. Separable Kvβ subunit domains alter expression and gating of potassium channels. *J. Biol. Chem.* 272:25824–25831.

Adda, S., B.K. Fleischmann, B.D. Freedman, M.F. Yu, D.W.P. Hay, and M.I. Kotlikoff. 1996. Expression and function of voltage-dependent potassium channel genes in human airway smooth muscle. *J. Biol. Chem.* 271:13239–13243.

Attali, B., F. Lesage, P. Ziliani, E. Guillemare, E. Honoré, R. Waldmann, J.-P. Hugnot, M.-G. Mattéi, M. Lazdunski, and J. Barhanin. 1993. Multiple mRNA isoforms encoding the mouse cardiac Kv1-5 delayed rectifier K^+ channel. *J. Biol. Chem.* 268:24283–24289.

Baukrowitz, T., and G. Yellen. 1996. Use-dependent blockers and exit rate of the last ion from the multi-ion pore of a K^+ channel. *Science.* 271:653–656.

Brandt, M.C., L. Priebe, T. Böhle, M. Südkamp, and D.J. Beuckelmann. 2000. The ultrarapid and the transient outward K^+ current in human atrial fibrillation. Their possible role in postoperative atrial fibrillation. *J. Mol. Cell. Cardiol.* 32:1885–1896.

Clément-Chomienne, O., K. Ishii, M.P. Walsh, and W.C. Cole. 1999. Identification, cloning and expression of rabbit vascular smooth muscle Kv1.5 and comparison with native delayed rectifier K^+ current. *J. Physiol.* 515:653–667.

Cushman, S.J., M.H. Nanao, A.W. Jahng, D. DeRubeis, S. Choe, and P.J. Pfaffinger. 2000. Voltage dependent activation of potassium channels is coupled to T1 domain structure. *Nat. Struct. Biol.* 7:403–407.

Dobrzynski, H., S.M. Rothery, D.D.R. Marples, S.R. Coppen, Y. Takagishi, H. Honjo, M.M. Tamkun, Z. Henderson, I. Kodama, N.J. Severs, and M.R. Boyett. 2000. Presence of the Kv1.5 K^+ channel in the sinoatrial node. *J. Histochem. Cytochem.* 48:769–780.

Fedida, D., B. Wible, Z. Wang, B. Fermini, F. Faust, S. Nattel, and A.M. Brown. 1993. Identity of a novel delayed rectifier current from human heart with a cloned K^+ channel current. *Circ. Res.* 73:210–216.

Fedida, D., N.D. Maruoka, and S. Lin. 1999. Modulation of slow inactivation in human cardiac Kv1.5 channels by extra- and intracellular permeant cations. *J. Physiol.* 515:315–329.

Gulbis, J.M., M. Zhou, S. Mann, and R. MacKinnon. 2000. Structure of the cytoplasmic β subunit - T1 assembly of voltage-dependent K^+ channels. *Science.* 289:123–127.

Hoshi, T., W.N. Zagotta, and R.W. Aldrich. 1991. Two types of inactivation in *Shaker* K^+ channels: effects of alterations in the carboxy-terminal region. *Neuron.* 7:547–556.

Hoshi, T., W.N. Zagotta, and R.W. Aldrich. 1994. *Shaker* potassium channel gating. I: transitions near the open state. *J. Gen. Physiol.* 103:249–278.

Jerng, H.H., M. Shahidullah, and M. Covarrubias. 1999. Inactivation gating of Kv4 potassium channels: Molecular interactions involving the inner vestibule of the pore. *J. Gen. Physiol.* 113:641–659.

Jiang, M., J. Tseng-Crank, and G.N. Tseng. 1997. Suppression of slow delayed rectifier current by a truncated isoform of KvLQT1 cloned from normal human heart. *J. Biol. Chem.* 272:24109–24112.

Jones, S.W., and T.N. Marks. 1989. Calcium currents in bullfrog sympathetic neurons. I. Activation kinetics and pharmacology. *J. Gen. Physiol.* 94:151–167.

Kerschensteiner, D., and M. Stocker. 1999. Heteromeric assembly of Kv2.1 with Kv9.3: effect on the state dependence of inactivation. *Biophys. J.* 77:248–257.

Klemic, K.G., C.C. Shieh, G.E. Kirsch, and S.W. Jones. 1998. Inactivation of Kv2.1 potassium channels. *Biophys. J.* 74:1779–1789.

Kobertz, W.R., and C. Miller. 1999. K^+ channels lacking the 'tetramerization' domain: implications for pore structure. *Nat. Struct. Biol.* 6:1122–1125.

Kobertz, W.R., C. Williams, and C. Miller. 2000. Hanging gondola structure of the T1 domain in a voltage-gated K^+ channel. *Biochemistry.* 39:10347–10352.

Kramer, J.W., M.A. Post, A.M. Brown, and G.E. Kirsch. 1998. Modulation of potassium channel gating by coexpression of Kv2.1 with regulatory Kv5.1 or Kv6.1 α-subunits. *Am. J. Physiol. Cell Physiol.* 274:C1501–C1510.

Kreusch, A., P.J. Pfaffinger, C.F. Stevens, and S. Choe. 1998. Crystal structure of the tetramerization domain of the *Shaker* potassium channel. *Nature.* 392:945–948.

Kuo, C.C., and B.P. Bean. 1993. G-protein modulation of ion permeation through N-type calcium channels. *Nature.* 365:258–262.

Lee, T.E., L.H. Philipson, A. Kuznetsov, and D.J. Nelson. 1994. Structural determinant for assembly of mammalian K^+ channels. *Biophys. J.* 66:667–673.

Li, M., Y.N. Jan, and L.Y. Jan. 1992. Specification of subunit assembly by the hydrophilic amino-terminal domain of the shaker potassium channel. *Science.* 257:1225–1230.

Loots, E., and E.Y. Isacoff. 2000. Molecular coupling of S4 to a K^+ channel's slow inactivation gate. *J. Gen. Physiol.* 116:623–636.

Lopez-Barneo, J., T. Hoshi, S.H. Heinemann, and R.W. Aldrich. 1993. Effects of external cations and mutations in the pore region on C-type inactivation of Shaker potassium channels. *Recept. Channels.* 1:61–71.

Marom, S., and L.F. Abbott. 1994. Modeling state-dependent inactivation of membrane currents. *Biophys. J.* 67:515–520.

Maruoka, N.D., D.F. Steele, B.P.Y. Au, P. Dan, X. Zhang, E.D.W. Moore, and D. Fedida. 2000. α-Actinin-2 couples to cardiac Kv1.5 channels, regulating current density and channel localization in HEK cells. *FEBS Letts.* 473:188–194.

Minor, D.L., Jr., Y.F. Lin, B.C. Mobley, A. Avelar, Y.N. Jan, L.Y. Jan, and J.M. Berger. 2000. The polar T1 interface is linked to conformational changes that open the voltage-gated potassium channel. *Cell.* 102:657–670.

Ogielska, E.M., W.N. Zagotta, T. Hoshi, S.H. Heinemann, J. Haab, and R.W. Aldrich. 1995. Cooperative subunit interactions in C-type inactivation of K channels. *Biophys. J.* 69:2449–2457.

Olcese, R., R. Latorre, L. Toro, F. Bezanilla, and E. Stefani. 1997. Correlation between charge movement and ionic current during slow inactivation in *Shaker* K^+ channels. *J. Gen. Physiol.* 110:579–589.

Overturf, K.E., S.N. Russell, A. Carl, F. Vogalis, P.J. Hart, J.R. Hume, K.M. Sanders, and B. Horowitz. 1994. Cloning and characterization of a $K_v1.5$ delayed rectifier K^+ channel from vascular and visceral smooth muscles. *Am. J. Physiol. Cell Physiol.* 267:C1231–C1238.

Panyi, G., Z. Sheng, L. Tu, and C. Deutsch. 1995. C-type inactivation of a voltage-gated K^+ channel occurs by a cooperative mechanism. *Biophys. J.* 69:896–903.

Patil, P.G., D.L. Brody, and D.T. Yue. 1998. Preferential closed-state inactivation of neuronal Ca^{2+} channels. *Neuron.* 20:1027–1038.

Pongs, O., T. Leicher, M. Berger, J. Roeper, R. Bähring, D. Wray, K.P. Giese, A.J. Silva, and J.F. Storm. 1999. Functional and molecular aspects of voltage-gated K^+ channel β subunits. *Ann. NY Acad. Sci.* 868:344–355.

Rehm, H., and M. Lazdunski. 1988. Purification and subunit structure of a putative K^+-channel protein identified by its binding properties for dendrotoxin I. *Proc. Natl. Acad. Sci. USA.* 85:4919–4923.

Rettig, J., S.H. Heinemann, F. Wunder, C. Lorra, D.N. Parcej, J.O. Dolly, and O. Pongs. 1994. Inactivation properties of voltage-gated K^+ channels altered by presence of β-subunit. *Nature.* 369: 289–294.

Sasaki, Y., K. Ishii, K. Nunoki, T. Yamagishi, and N. Taira. 1995. The voltage-dependent K^+ channel (Kv1.5) cloned from rabbit heart and facilitation of inactivation of the delayed rectifier current by the rat β subunit. *FEBS Lett.* 372:20–24.

Schaffer, P., B. Pelzmann, E. Bernhart, P. Lang, J.E. Lokebo, H. Mächler, B. Rigler, and B. Koidl. 1998. Estimation of outward currents in isolated human atrial myocytes using inactivation time course analysis. *Pflügers Arch.* 436:457–468.

Schoppa, N.E., and F.J. Sigworth. 1998. Activation of *Shaker* potassium channels I. Characterization of voltage-dependent transitions. *J. Gen. Physiol.* 111:271–294.

Sewing, S., J. Roeper, and O. Pongs. 1996. Kvβ 1 subunit binding specific for Shaker-related potassium channel α subunits. *Neuron.* 16:455–463.

Shen, N.V., and P.J. Pfaffinger. 1995. Molecular recognition and assembly sequences involved in the subfamily-specific assembly of voltage-gated K^+ channel subunit proteins. *Neuron.* 14:625–633.

Shen, N.V., X. Chen, M.M. Boyer, and P.J. Pfaffinger. 1993. Deletion analysis of K^+ channel assembly. *Neuron.* 11:67–76.

Strang, C., S.J. Cushman, D. DeRubeis, D. Peterson, and P.J. Pfaffinger. 2001. A central role for the T1 domain in voltage-gated potassium channel formation and function. *J. Biol. Chem.* 276: 28493–28502.

Tamkun, M.M., K.M. Knoth, J.A. Walbridge, H. Kroemer, D.M. Roden, and D.H. Glover. 1991. Molecular cloning and characterization of two voltage-gated K^+ channel cDNAs from human ventricle. *FASEB J.* 5:331–337.

Tu, L.W., V. Santarelli, Z.F. Sheng, W. Skach, D. Pain, and C. Deutsch. 1996. Voltage-gated K^+ channels contain multiple intersubunit association sites. *J. Biol. Chem.* 271:18904–18911.

VanDongen, A.M.J., G. Frech, J.A. Drewe, R.H. Joho, and A.M. Brown. 1990. Alteration and restoration of K^+ channel function by deletions at the N- and C-termini. *Neuron.* 5:433–443.

Van Wagoner, D.R., A.L. Pond, P.M. McCarthy, J.S. Trimmer, and J.M. Nerbonne. 1997. Outward K^+ current densities and Kv1.5 expression are reduced in chronic human atrial fibrillation. *Circ. Res.* 80:772–781.

Wang, Z., B. Fermini, and S. Nattel. 1993. Delayed rectifier outward current and repolarization in human atrial myocytes. *Circ. Res.* 73:276–285.

Wang, Z., J.C. Hesketh, and D. Fedida. 2000. A high-Na^+ conduction state during recovery from inactivation in the potassium channel Kv1.5. *Biophys. J.* 89:23–45.

Xu, J., W.F. Yu, Y.N. Jan, L.Y. Jan, and M. Li. 1995. Assembly of voltage-gated potassium channels. Conserved hydrophilic motifs determine subfamily-specific interactions between the α-subunits. *J. Biol. Chem.* 270:24761-24768.

Zagotta, W.N., T. Hoshi, J. Dittman, and R.W. Aldrich. 1994a. *Shaker* potassium channel gating. II: Transitions in the activation pathway. *J. Gen. Physiol.* 103:279–319.

Zagotta, W.N., T. Hoshi, and R.W. Aldrich. 1994b. *Shaker* potassium channel gating. III: Evaluation of kinetic models for activation. *J. Gen. Physiol.* 103:321–362.

Zhou, M., J.H. Morais-Cabral, S. Mann, and R. MacKinnon. 2001. Potassium channel receptor site for the inactivation gate and quaternary amine inhibitors. *Nature.* 411:657–661.